Christopher Grenke's ESFD research program · November 23, 2026

NGC 2403 and the missing outer speed

At 4.97 kpc the shared core equation predicts 121.6 km/s and the gas moves at 121. At 20.87 kpc it predicts 114.9 and the gas moves at 134 ± 3.1. The equation levels off too early to compensate for the falling contribution of the observed stars and gas.

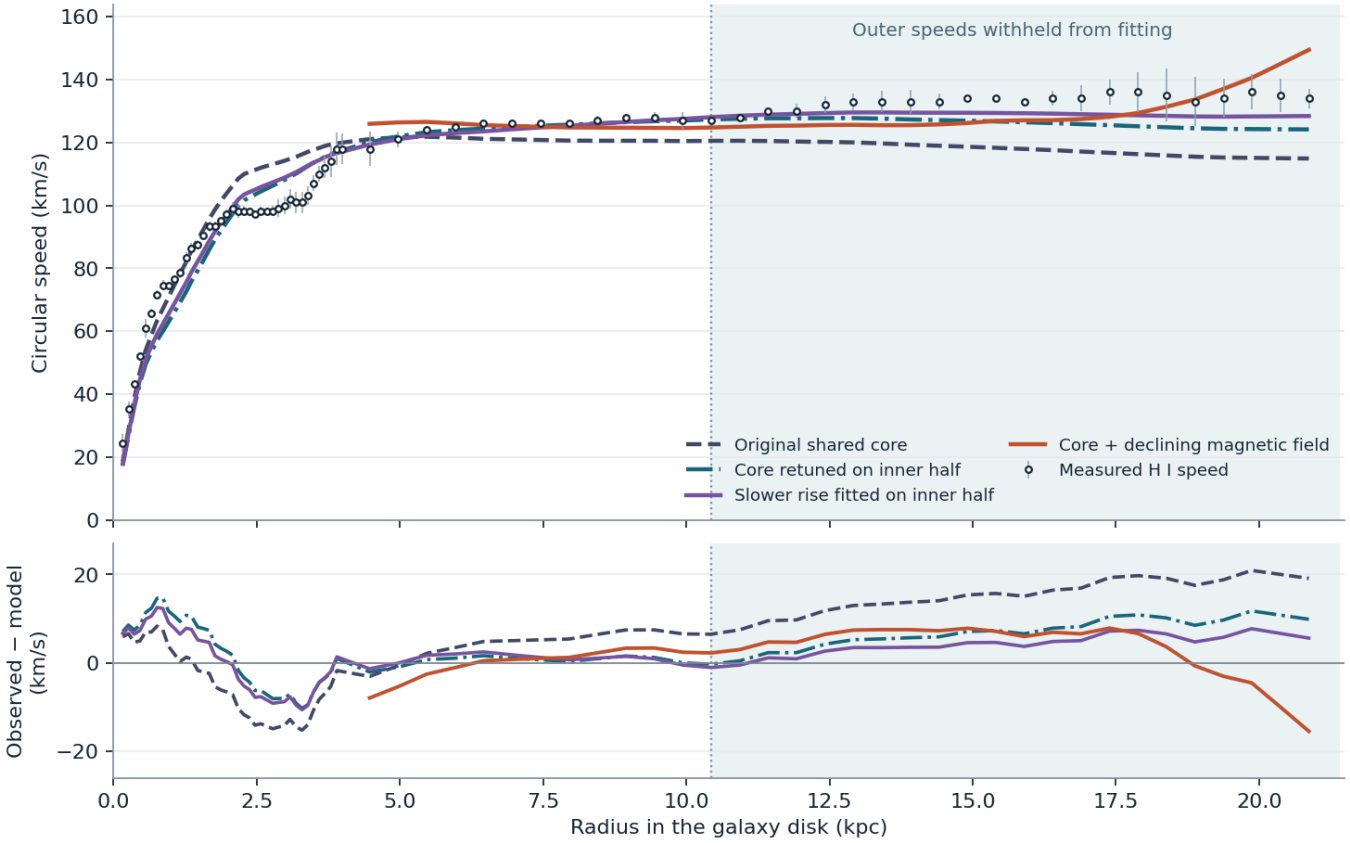

Figure 1. The shaded region contains the 21 radii held out of the local fits. In the lower panel, positive values mean the galaxy rotates faster than the equation predicts. The magnetic curve uses measured H I columns, an assumed 1 kpc gas scale height, and an inner-disk estimate of the field amplitude.

The original shared core missed the outer points by 16.0 km/s root-mean-square. Retuning its two coefficients cut that to 7.8. A slower-rising core gave 4.9. A magnetic correction gave 7.0 under the primary assumptions, yet overshot the last measurement by 15.5 km/s.

A radio reanalysis shows a spiral field pattern. A separate compilation estimates a galaxy-wide total field of 5.7 μG. The crucial quantity is the strength *and radial change* of the field circling the galaxy in the 20–22 kpc gas ring. The available observations do not determine either quantity there. [1–5]

What goes wrong in the two equations

The gray “stars and gas” curve in the original figure gives the speed expected from the measured baryonic mass distribution. The project’s orange spin–entropy flux curve and teal revised core add a contribution to *squared* speed. The galaxy’s falling baryonic contribution makes the radial shape of that addition decisive. [1]

$$v_{core}^2 = v_{bar}^2 + \sqrt{(G\, M_{bar}\, a_*)}\; r^2 / [r^2 + (\eta R_d)^2]$$

Here r is radius, G the gravitational constant, M_{bar} the adopted stars-plus-gas mass, R_d the stellar disk scale length, a_* an acceleration scale and ηR_d the core radius. For this galaxy the inputs are 9.275 × 10^9 solar masses and 1.39 kpc. The shared coefficients are $a_* = 0.920 \times 10^{-10}$ m/s² and η = 1.352. Inner tuning gives 1.383×10^{-10} and 2.233, expanding the core from 1.88 to 3.10 kpc.

$$v_{flux}^2 = v_{bar}^2 + (G\, M_{bar}/r)\; A\; (r/R_d)^2\; \exp[-r/(\lambda\, R_d)]$$

This is the archived computable SEFD spin–entropy flux prescription. Its extra term scales as $r \exp[-r/(\lambda R_d)]$, so it peaks at λR_d and then falls. The frozen and retuned peak radii are 9.19 and 13.86 kpc. The revised core flattens instead. Both eventually supply too little inward acceleration here. The slower-rise comparison uses the profile $1 - \arctan(x)/x$, with $x = r/(\eta R_d)$. It also occurs in a pseudo-isothermal halo. Rotation fits alone cannot identify which physics produced that shape.

Radius	Observed	Stars + gas	Shared core	Extra v² required	Extra v² supplied
4.97 kpc	121.0	74.1	121.6	9,157	9,311
20.87 kpc	134.0	51.4	114.9	15,310	10,556

Speeds are in km/s. Squared speeds are in (km/s)². At the endpoint the missing 4,754 (km/s)² corresponds to 7.38×10^{-12} m/s² of inward acceleration. The speed gap itself is 19.1 km/s.

Holding the published line-of-sight speed and the model fixed, correcting the last point by inclination alone would require $\sin(i) = 1.039$. That simple adjustment is impossible. A varying disk position angle, distorted gas, incomplete azimuthal sampling or a changed mass model can still shift a fitted outer speed. The original H I analysis identified a separate, slower gas component. [1, 2, 6]

How much of the outer curve can we predict?

I froze distances, inclinations, baryonic decompositions and galaxy-fold assignments from the preceding master. For NGC 2403 the adopted distance is 3.16 Mpc and the inclination is 63°. Measured speeds at 52 radii through 10.435 kpc determined local coefficients. I scored all 21 farther radii with no additional velocity fitting. The previous diagram had already revealed the endpoint miss, so this is a retrospective extrapolation test. [1]

Model and parameter source	Outer RMSE	Speed at 20.87 kpc
Stars + gas + original flux, shared parameters	19.89	102.19
Stars + gas + original flux, inner fit	8.63	119.83
Revised core, shared parameters	15.98	114.90
Core, amplitude retuned	14.15	116.85
Core, amplitude and size retuned	7.80	124.15
Slower-rise profile, two inner-fit parameters	4.90	128.40
Constant from last three inner speeds	6.64	127.00
Radial acceleration relation, training-galaxy calibration	9.34	124.00
Shared NFW halo calibration from the archive	14.00	114.90
Shared Burkert halo calibration from the archive	21.11	105.23
Core + inner-fit declining field, whole-ring gas	7.04	149.46
Measured endpoint	—	134.00 ± 3.12

All speeds and errors are in km/s. RMSE is the square root of the average squared speed error. The shared curves were calibrated with other galaxies. Each occupied 1 kpc bin has equal total weight in the local training loss. The magnetic fit uses the 13 training radii at or above 4 kpc. Frozen halo rows describe these specific calibrations.

The fit depends on how much of the disk we already know. Training through only 5 kpc gives outer errors of 23.68 for the retuned core and 19.30 for the slower rise. Training through 40% gives 8.14 and 4.62. At 60% the errors are 7.06 and 4.47, and a simple constant scores 4.26. Fitting all 73 speeds yields a final 133.10 for the slow profile. That last value uses the measurements it describes.

Where the radio observations actually reach

Heald and colleagues detected diffuse polarized synchrotron emission in NGC 2403, typically 30–50 μJy per beam after smoothing, with brighter patches near 100 μJy per beam. Their integrated polarized flux was 28 ± 5 mJy. Drzazga's 2014 reprocessing of the same observations recovered an asymmetric spiral pattern and a Faraday-depth map, with most polarization on the western side. The latter used 765 frequency channels and a 49.5″ × 45″ beam. [3, 4]

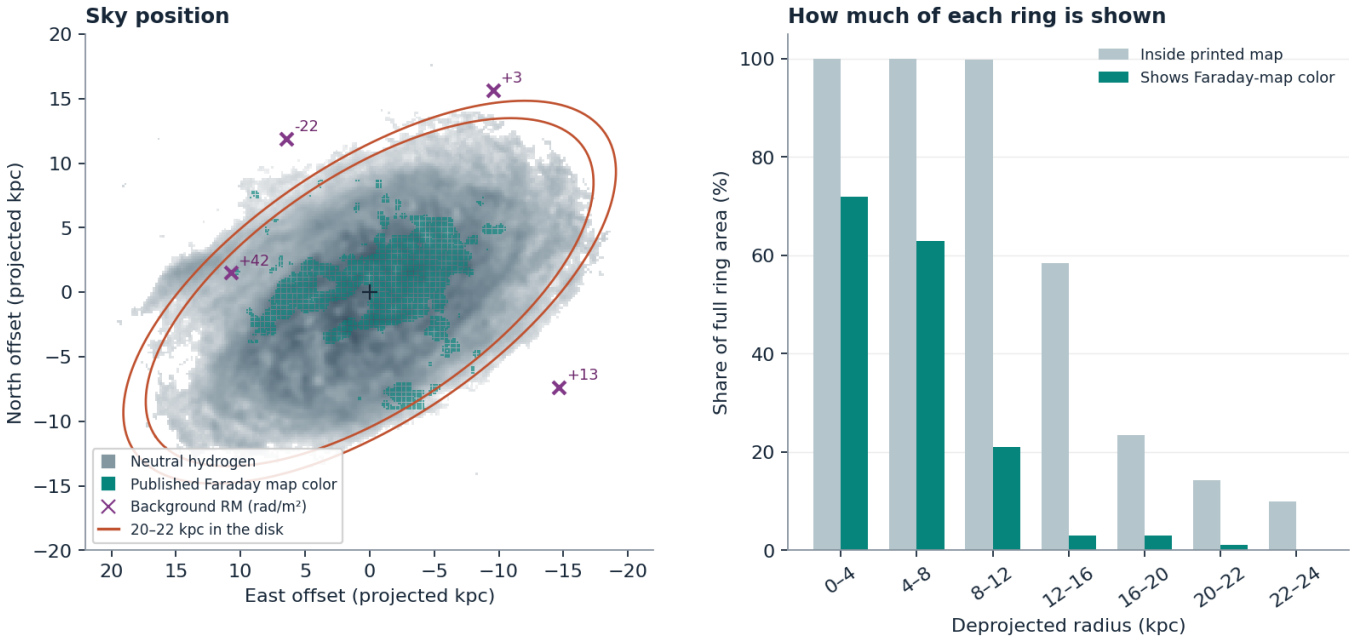

Figure 2. East is on the left. The pale gray disk is measured H I. Teal marks colored pixels in Drzazga's Fig. A.3 as registered from its printed coordinate ticks. They indicate where peak Faraday depth is displayed. The purple crosses are distinct background sources. Blank areas can result from sensitivity, depolarization or the figure boundary.

In the adopted geometry, the printed map includes approximately 14% of the area of the 20–22 kpc ring. About 1.1% of the full ring shows plotted Faraday-depth color. These pixels lie near the projected minor axis, where circular rotation produces little line-of-sight velocity. Changing inclination by ±3° and position angle by ±5° gives 0–2.7% displayed color for the full ring. This estimate measures published figure coverage. The original survey field of view can extend farther.

The consolidated RM catalog has a +42 ± 2 rad/m² background-source measurement at a projected disk radius of 17.95 kpc. An independent NVSS value is +3.3 ± 15.4 at 23.70 kpc. The searched RM catalog has zero entries in the 20–22 kpc ring. Its one NVSS catalog *continuum* component has polarized flux 0.49 ± 0.51 mJy, below even a 3σ selection. The three Heald sightlines also underlie the quoted Milky Way foreground of +11 ± 30 rad/m². Subtracting it as an independent measurement would double-count information. [3, 7, 8]

What a magnetic force would have to do

Relativistic electrons spiraling in a magnetic field emit polarized radio waves. Their polarization tells us about field orientation and about material crossed on the way here. An ordered field can also bend and exert tension on magnetically coupled gas. Inward tension competes with the radial magnetic-pressure gradient. Detecting radio waves, even polarized ones, does not establish wave interference or the size and direction of this force. [3, 4, 9]

> $\Delta v_B^2 = [B_\varphi^2/(\mu_0\rho)]\,[1 + d \ln |B_\varphi|/d \ln r]$

This steady, axisymmetric illustration keeps a toroidal field, B_φ, and gas mass density ρ. A slowly declining field can add inward force. If $B_\varphi \propto 1/r$ the tension and pressure cancel. A steeper local decline reverses the sign. Vertical and radial fields, random-field pressure, cosmic rays, gas pressure, spiral shocks and departures from steady motion can all change the calculation. Earlier MHD work found that outer-disk fields can impede rotation. [9]

From the HALOGAS 20–22 kpc ring, the coarser map gives a face-on neutral hydrogen column of 2.33 × 10^{19} atoms/cm², or 0.187 solar masses/pc² of H I. The higher-resolution map gives 1.48 × 10^{19}. The fractions of positive pixels in the source-masked maps are 44% and 21%. Detected pixels alone give 5.27 and 6.89 × 10^{19}. These are two different ways of averaging patchy gas. Unseen gas below the mask and other phases can raise the relevant mass density. [2]

For a Gaussian layer with a 1 kpc vertical standard deviation, $n_H = N_{HI,face}/(\sqrt{(2\pi)}\, h)$ gives 0.0030 hydrogen atoms/cm³ for the coarse whole-ring mean. Taking $\rho = 1.4\, m_p n_H$, the table gives the local field needed to close the old core's entire endpoint gap.

Gas sampled in coarse map	Locally constant Bφ	Bφ declines as $r^{-1/2}$
Whole ring	2.05 μG	2.91 μG
Detected pixels	3.09 μG	4.37 μG

Chyży and colleagues estimate 5.7 μG for this galaxy's *average total* field under synchrotron energy equipartition. Its presence makes an outer-field test meaningful. The local circling component and its slope at 20.87 kpc remain unknown. At fixed column the required field varies as $1/\sqrt{h}$. Changing h from 0.5 to 1.5 kpc moves the coarse whole-ring target for the declining field from 4.11 to 2.37 μG. [5]

Putting the field into the velocity prediction

I fixed the old core, tested $B_\varphi(r) = B_{10}(r/10\ \mathrm{kpc})^s$ with $s = 0$ or $-½$, and inferred only the nonnegative amplitude from speeds between 4 and 10.435 kpc. The measured hydrogen columns at each outer radius enter the prediction. All outer velocities stay out of the fit. The primary case uses the coarse whole-ring column and a 1 kpc height.

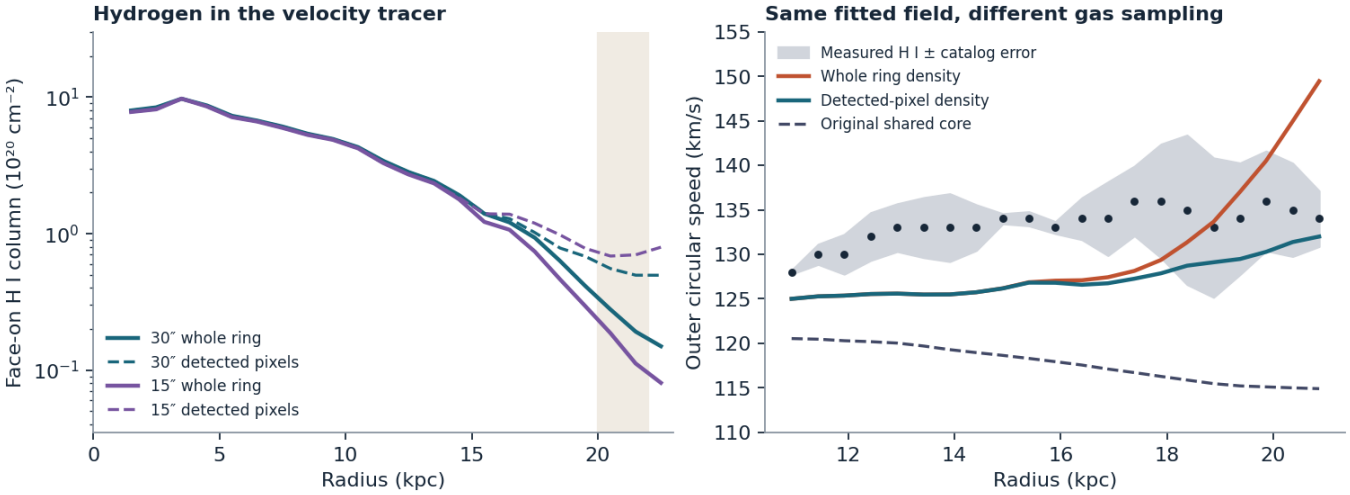

Figure 3. Both solid velocity curves use the same magnetic amplitude fitted in the inner disk. They diverge in the outskirts because the two gas-density averages diverge there. The shaded observed range uses the quoted point errors only.

A constant 5.12 μG field predicts 203.1 km/s at the tip and an outer RMSE of 24.53. A field falling as $r^{-½}$ fits B_{10} = 5.97 μG, scores 7.04 and reaches 149.46. The same declining field using only pixels with detected gas gives 132.00 at the endpoint and an outer RMSE of 6.33. The higher-resolution whole-ring calculation reaches 164.61. Choosing the gas sample because it matches 134 would use the answer to define the model.

An exploratory test ties B_{10} to the published 5.7 μG disk mean with no velocity fitting. At an assumed fraction of one half and slope $-½$ the last prediction is 123.63. At fraction one it is 146.73. The unknown fraction prevents a unique prediction from the radio measurement.

As a thickness sensitivity, the included calculation uses the flaring profile digitized from the 2024 Bacchini et al. figure. It is a hydrostatic modeling result, reaching 18.6 kpc after distance rescaling. Holding its last height, roughly 0.81 kpc, beyond that radius gives 183.6 on the coarse whole-ring declining-field test. The journal lists a 2026 corrigendum whose implications for that profile were unverified here. The primary fixed-height results are independent of this source. [10]

Can the result travel to other galaxies?

I applied NGC 2403's inner-fit coefficients without adjustment to 245 separate PROBES galaxies and repeated the comparison on 130 other SPARC galaxies. The external sample contributes 16,120 velocity entries. Each galaxy counts once in the median. Both cohorts come from the previous release's eligibility and cross-match rules. PROBES uses different baryonic inputs and samples a different distribution of radii. [1, 11]

Model applied to other galaxies	PROBES median RMSE	Improved / 245	Other SPARC median
Original shared core	29.92	—	12.55
NGC 2403 amplitude alone	29.02	176	12.38
NGC 2403 amplitude and core size	34.01	36	13.88
NGC 2403 slower-rise coefficients	32.66	40	14.11

Units are km/s. The paired median change for the two-coefficient core is +5.55 km/s, with a galaxy-bootstrap 95% interval of +4.97 to +5.98. A positive change means greater error. The amplitude-only change was promising on PROBES, though it improved only 58 of the 130 other SPARC galaxies.

A different question is whether each galaxy's own inner speeds help predict its outer speeds. On the 242 PROBES objects with adequate sampling, this cut median outer error from 26.76 to 23.31 km/s and improved 141 of them. A flat extrapolation gave 24.77. In 60 galaxies the two-parameter fit reached a parameter bound. For 94 eligible other SPARC disks, the corresponding errors were 12.54, 9.24 and 10.01.

I also applied NGC 2403's fitted magnetic amplitude and slope to two other HALOGAS disks, using each galaxy's own hydrogen map and the same assumed 1 kpc height. These were a small direct check on the field prescription. Their old curves already overpredicted the endpoint, so adding an inward force pushed both farther from the measurements.

Disk and sampled range	Radii	Old core RMSE	Declining field RMSE
NGC 3198, 11.04–20.05 kpc	6	7.30	9.45
NGC 5055, 11.49–20.07 kpc	4	34.33	36.62

With no velocity fitting, substituting each control's own published total-field estimate, 4.9 and 8.5 μG, as the circling component at 10 kpc also worsens both errors. A common correction needs an independently observable way to predict its sign and amplitude. [2, 5]

An observation that could decide the case

Target both ends of the projected major axis from 15 to 23 kpc. At 20.87 kpc the two centers are (RA, Dec) = (114.96745°, +65.38907°) southeast and (113.44848°, +65.81224°) northwest in J2000 coordinates, 22.70′ from the center. Add comparison pointings near the minor axis and beyond the disk. Obtain sensitive broadband Stokes Q and U, multi-frequency synchrotron intensity, and a grid of background rotation measures. Sensitivity to diffuse angular scales, thermal-emission removal and a model for cosmic-ray electrons matter for converting brightness to field strength. Foreground rotation, turbulent fields and the density of free electrons matter for interpreting Faraday depth. Measure gas thickness or constrain it from independent observations and fit the projected H I velocity field with a varying disk geometry. [3, 4, 6, 9]

The specific prediction is a positive inward contribution of roughly 7.4×10^{-12} m/s² at 20.87 kpc relative to the shared core. Freeze the reconstructed field and gas-density model before computing gas speeds in the reserved sectors. If the independently constrained circling field falls locally as $1/r$ or faster, this axisymmetric term cannot supply that positive gap. Compare both disk sides and compare young or old stellar tracers where feasible. A gas-specific force and an additional gravitational potential can have different observational signatures.

The new release includes the gas maps at two resolutions, magnetic catalog positions, the registered published map support, all model predictions and source code. It also includes an explicit inverse calculation. For an assumed density it integrates $\mathrm{d}(r^2 B_\varphi{}^2)/\mathrm{d}r = 2r\,\mu_0 \rho \Delta v^2$ in consistent units. A boundary field must be supplied. This reconstruction uses the velocity data and yields possible profiles for a later measurement to challenge.

Fixed-geometry checks on the 20–22 kpc H I velocity maps give about 127.4 and 130.1 km/s at the two beam sizes. Changing the position angle by 5° moves the coarse estimate to 135.8 or 139.5. This annular first-moment calculation and the catalog’s last point sample gas differently and share the same underlying VLA observations. A full cube fit and independent stellar velocities would improve the dynamical comparison. [2, 6]

The galaxy test evaluates an empirical galactic rotation law and an ordinary magnetic gas force. A favorable result could guide the galaxy branch of ESFD. A connection to the unified spin–field equations requires a derivation of the field law from those equations and independent predictions in the other branches.

Sources and reproducibility

1. SPARC data and mass models. Lelli, McGaugh & Schombert (2016). Rotation speeds, baryonic decomposition, distance and inclination.
2. HALOGAS Data Release 1. Heald and collaborators. Native column-density and velocity FITS. NGC 2403 uses archival VLA AS649 observations from Fraternali et al. (2002).
3. Westerbork SINGS II. Heald, Braun & Edmonds (2009), §4 and Table 1. Diffuse polarization, integrated flux and background lines of sight.
4. Galactic magnetized plasma exposed to winds and tidal interactions. Drzazga (2014), dissertation Appendix A, Figs. A.2–A.3. Re-imaging of the same visibility data.
5. What drives galactic magnetism?. Chyży et al. (2017), A&A 603, A121. Galaxy-average equipartition fields from Table A.1.
6. THINGS high-resolution rotation curves. de Blok et al. (2008). Comparison of NGC 2403 curves and outer-ring geometry.
7. RMTable version 1.2.0. Van Eck et al. Consolidated rotation-measure catalog, including the Taylor et al. NVSS measurements. The LoTSS DR2 radio-polarization TAP catalog also returned zero entries within 2°.
8. 1.4 GHz NRAO VLA Sky Survey. Condon et al. (1998). Cataloged continuum sources and integrated polarized flux within 45 arcmin.
9. Do magnetic fields influence gas rotation in galaxies?. Elstner, Beck & Gressel (2014). Radial force from tension and pressure in galactic gas disks.
10. 3D local instability of cold gas disks. Bacchini et al. (2024), Fig. B.6. The optional sensitivity uses that edition. 2026 corrigendum DOI 10.1051/0004-6361/202662855e.
11. PROBES I rotation curves and photometry. Stone et al. (2022), survey release. The selected compact sample follows the preceding ESFD observational release.

This research made use of data from WSRT HALOGAS-DR1. The Westerbork Synthesis Radio Telescope is operated by ASTRON (Netherlands Institute for Radio Astronomy) with support from the Netherlands Foundation for Scientific Research NWO.

The research package contains the analysis choices recorded before fitting, input data, eight original HALOGAS FITS products, published-map digitization coordinates, 24-sector gas summaries, per-radius speed predictions, per-galaxy transfer scores and an offline Python runner. Assumptions and figure-derived quantities are identified in the tables and in the methods above.